



Effect of nanoparticles on electrical properties of PVDF-based Mg²⁺ ion conducting polymer electrolytes

NIDHI , SANDHYA PATEL* and RANVEER KUMAR

Department of Physics, Dr. Harisingh Gour Vishwavidyalaya Sagar, Sagar 470003, India

*Author for correspondence (sandhyaparipalak@gmail.com)

MS received 12 March 2020; accepted 11 November 2020

Abstract. Polyvinylidene fluoride (PVDF)-based nanocomposite polymer electrolyte (NCPE) thin films for electrochemical applications have been synthesized by solution cast technique. NCPEs have 70PVDF:30Mg(NO₃)₂ solid polymer electrolyte (SPE) with conductivity $\sim 7.3 \times 10^{-8}$ S cm⁻¹ as phase-I and various nanoparticles as phase-II, dispersed in SPE for enhancement in its conductivity. These NCPE films were characterized by Fourier transform infrared (FTIR) spectroscopy, X-ray diffraction (XRD) and impedance spectroscopic techniques to study the structural and electrical properties. XRD and FTIR studies of film confirms formation of complexes. From composition and temperature dependence of conductivity analysis, we have obtained an optimum conducting composition of NCPE, i.e., 70PVDF:30Mg(NO₃)₂:3ZnO with conductivity $\sigma = 3.7 \times 10^{-4}$ S cm⁻¹. Ionic transport number ($t_{\text{ion}} = 0.99$) have been calculated from Wagner's dc polarization technique. Electrochemical cell has been fabricated using cell configuration MglNCPE|carbon cell and various cell parameters have been calculated from their discharge characteristics.

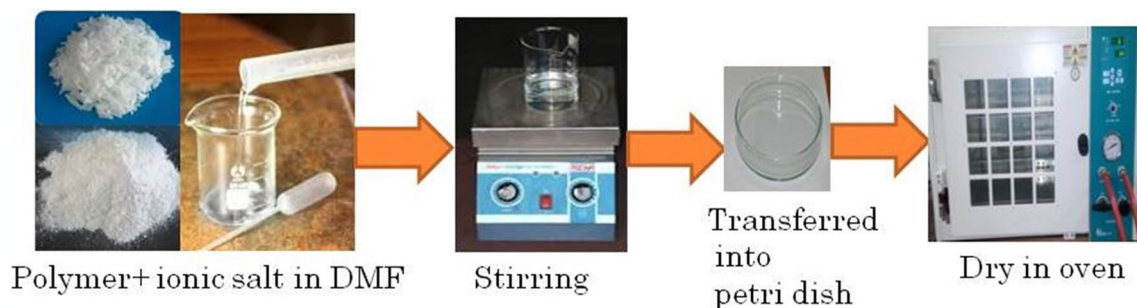
Keywords. Polyvinylidene fluoride; transport number; DSC-TGA; discharge characteristics.

1. Introduction

Since 1991, lithium ion batteries are potential candidates for power sources in portable electronics (camera, camcorder, electric vehicles, smart phones, laptops and calculators and so on) [1]. In batteries, electrolytes decide current density, energy density, power density, time stability, long shelf life, small shelf discharge capacity, good capacity of retention, low environment pollution, compatibility with electrode material, safety and so on [2–5]. Remarkable improvements have been made in the field of electrolytes used for battery applications [6–10]. Sundaram and Subramania [11] reported a gel polymer electrolyte, i.e., PVDF-HFP:PVA:LiClO₄ with conductivity value $\sigma = 7.94 \times 10^{-3}$ S cm⁻¹ at room temperature and proposed their system for rechargeable Li ion batteries. Li ion-based electrolytes are highly reactive in nature and due to their high cost research has been focused on the concept of magnesium ion conducting electrolytes [12–16]. Polu and Kumar [17] reported magnesium ion conducting polymer electrolyte synthesized by solution cast technique and tested for battery properties in cell configuration MglPVA-PEG-Mg(NO₃)₂|carbon cell and MglPEG-Mg(CH₃COO)₂-Al₂O₃|carbon cell [18] with ionic conductivity $\sim 9.63 \times 10^{-5}$ and 3.45×10^{-6} S cm⁻¹, respectively. PVDF-based magnesium ion conducting gel polymer electrolyte reported by Pandey and Hashmi [19] have conductivity value $\sim 3.4 \times 10^{-3}$ S cm⁻¹ at 20°C and

discharge capacity of 200 mAh g⁻¹ calculated from discharge characteristics for test cell fabricated in configuration of MglPVDF-HFP:Mg(CF₃SO₃)₂:EMITf|MoO₃. EMITf denotes ionic liquid: 1-ethyl-3-methylimidazoleium trifluoromethanesulphonate. They suggest Mg ion in place of Li ion because it has comparable size, possesses good electrical properties, low cost material due to presence in large amount in our earth crust, safer, negative electrode potential, i.e., -2.3 V vs. standard hydrogen electrode, high charge density and so on [12,13]. It has been reported by various researchers for magnesium battery application in future, which gives efficiency nearly same as to that of lithium in terms of current and energy density, with Mglpolymer electrolyte|cathode-carbon cell or MgMn₂O₄ or MoO₃ etc. [14–16].

Solid polymer electrolytes (SPEs) are safe to use but they have low conductivity values, so by addition of plasticizer into SPE (gel polymer electrolyte) or dispersion of ceramic fillers into SPE (composite polymer electrolyte/nanocomposite polymer electrolyte (NCPE)—when filler size is in nano range), ionic conductivity can be improved [20]. In 2015, Priya *et al* [21] reported ZnO dispersed NCPE system: PMMA-PEG/nZnO/KI/I₂ ($\sigma = 3.28 \times 10^{-5}$ S cm⁻¹ at room temperature) used for conversion of sunlight into electricity using dye-sensitized solar cells (DSSCs), prepared by solution casting technique. ZnO nanoparticles used by them have been prepared by sol-gel method. They concluded that dispersion of ZnO nanoparticles improve



Scheme 1. Schematic illustration of preparation steps of polymer electrolyte.

ionic conductivity as well as mechanical strength. Field emission scanning electron microscopy study confirms the presence of two distinct phases, the first phase due to original polymer matrix (crystalline) and the second is amorphous area consisting of polymer subunit held together forming straight long chain along which ZnO nanoparticles of 20 nm are distributed.

In 2016, Johnsi and Suthanthiraraj [22], reported CeO_2 dispersed polymer electrolyte system (75 wt% PVDF-co-HFP:25 wt% ZnTf-5 wt% CeO_2 with ionic conductivity $3 \times 10^{-4} \text{ S cm}^{-1}$) prepared by solution casting technique and tested their system for eco-friendly zinc rechargeable battery with decomposition potential from 2.4 to 2.7 V. Prabakaran *et al* [23] reported a system of NCPE, i.e., PEO(6.25)-PVDF-HFP(18.75)- LiClO_4 (8)-PC(67)- BaTiO_3 (6) ($\sigma = 6 \times 10^{-3} \text{ S cm}^{-1}$ at room temperature) with LiFePO_4 /CPE/Li coin cell assembly for Li-battery applications. Hema *et al* [24] reported NCPE-80PVA:20PVDF:15 LiCF_3SO_3 :4 TiO_2 (ionic conductivity $\sigma = 3.7 \times 10^{-3} \text{ S cm}^{-1}$ at 303 K), prepared by the universal solution casting technique.

From literature survey, it reveals that nanoparticles (Al_2O_3 , MgO , ZnO, TiO_2 , CuO, SiO_2 , etc.) dispersion in SPE enhances its ionic conductivity in 2–3 order, mechanical, thermal and electrochemical stability. In our present study, PVDF as host polymer, $\text{Mg}(\text{NO}_3)_2$ as ionic salt and ZnO, TiO_2 and Al_2O_3 nanoparticles as dispersoid are used and thin films of NCPE has been synthesized by solution casting method [25,26]. Zinc oxide nanoparticles have good carrier mobility property in comparison with MgO nanoparticles and ZnO nanoparticles are transparent for visible light, so NCPE synthesized having ZnO dispersed in it can also be used in solar cell applications or optoelectronic devices [27–30].

In our earlier work, we have reported a system of NCPE 70PVDF:30 $\text{Mg}(\text{NO}_3)_2$:3 MgO NCPE, which has good ionic conductivity of order of $10^{-4} \text{ S cm}^{-1}$ and thermally stable [13]. FTIR, transport and discharge characteristics of 70PVDF:30 $\text{Mg}(\text{NO}_3)_2$:3 MgO are reported in this paper. In the present work, we have studied the effect of dispersion of ZnO, TiO_2 and Al_2O_3 nanoparticles on electrical conductivity of SPE and electrochemical properties of NCPE. In optimum conducting composition (OCC) of SPE, i.e., 70PVDF:30 $\text{Mg}(\text{NO}_3)_2$ system, x wt% of ZnO, TiO_2 and Al_2O_3 nanoparticles (where

$x = 0, 1, 2, 3, 4$, etc. in wt%) have been dispersed. NCPE films have been prepared by solution cast method. X-ray diffraction (XRD), Fourier transform infrared (FTIR) analysis, transport parameter measurement and battery discharge characteristics of NCPE have been studied.

2. Experimental

The polymer PVDF, ionic salt $\text{Mg}(\text{NO}_3)_2$ and ZnO, titania (TiO_2) and alumina (Al_2O_3) nanoparticles (size $< 50 \text{ nm}$, MW = 81.38, 79.8 and 101.96, Aldrich, USA) were used as starting material for synthesis purpose. Solution casting method was used for synthesis. Scheme 1 shows synthesis process route involved for polymer electrolyte development.

$\text{Mg}(\text{NO}_3)_2$ salt was dried in oven for 24 h to remove moisture. Then appropriate amount of all chemicals were weighted and dissolved in DMF and then stirred for ~ 24 h at 50°C to obtain homogeneous solution. Then cast obtained as solution in Petri dish was dried for ~ 72 h in oven maintained at 50°C to obtain freestanding film. Carbon, iodine and KI are used for preparing carbon cell. Magnesium metal used for preparing test cell with cell configuration $\text{Mg}|\text{polymer electrolyte}|\text{carbon cell}$ (C+ I_2 +electrolyte in 5:5:1 ratio).

Structural characterization of thin films of NCPE were performed by XRD (Bruker, D8 Advance X-ray diffractometer, $\text{CuK}\alpha$ source $\lambda = 1.54 \text{ \AA}$), transport property study were done by impedance spectroscopy (HIOKI, model no. 3532-50) by LCR Bridge and Wagner's dc polarization method, respectively. FTIR spectra were obtained from (Bruker, alpha-II) FTIR spectrophotometer in frequency range $500\text{--}4000 \text{ cm}^{-1}$. Battery testing of electrolytes were done by analysing discharge characteristics.

3. Results and discussion

3.1 Studies on ionic conductivity of PVDF: $\text{Mg}(\text{NO}_3)_2$:ZnO and PVDF: $\text{Mg}(\text{NO}_3)_2$: TiO_2 NCPEs

Figure 1 shows 'Log σ - x ' plot of NCPE thin films with varying concentration of ZnO or TiO_2 nanoparticles in

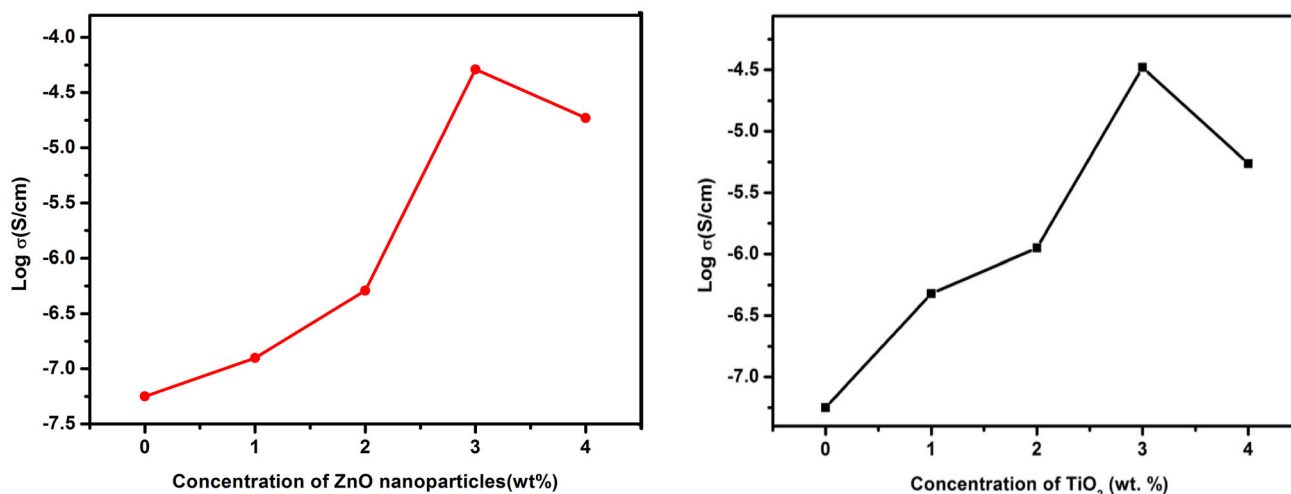


Figure 1. ‘Log σ - x ’ plot of NCPE thin films with varying concentrations of ZnO or TiO₂ nanoparticles in 70PVDF:30Mg(NO₃)₂ at room temperature.

70PVDF:30Mg(NO₃)₂ at room temperature to improve in its conductivity value. It was observed that the ionic conductivity increases on increasing the concentrations of nano-filler, which may be due to (a) ceramic particle addition in amorphous phase in polymer electrolyte, which provides new kinetic pathways and (b) ceramic particles act as catalyst or nucleation centre, which provide their surface for formation of minute crystallite [31]. The enhancement in the ionic conductivity value ($\sigma_{rt} = 5.22 \times 10^{-5}$ and 1.01×10^{-5} S cm⁻¹) was observed for 3 wt% of ZnO or TiO₂ dispersed in 70PVDF:30Mg(NO₃)₂ ($\sigma_{rt} = 7.3 \times 10^{-8}$ S cm⁻¹) polymer electrolyte system, respectively. On further enhancement in nanoparticles concentration, the ionic conductivity value is reduced and this may be due to formation of ion pairs and ion triplet, which retard the ion mobility [32–34]. Similar behaviour was observed for TiO₂ dispersed system.

3.2 XRD study

Figure 2 illustrates the XRD patterns of prepared SPE, i.e., 70PVDF:30Mg(NO₃)₂ and NCPE dispersed with different concentrations of ZnO or TiO₂ nanoparticles in SPE. From XRD profiles of different NCPE films, it was observed that a broad peak around 20.3° found to decrease in intensity. Peaks at 31.73°, 34.4°, 36.2°, 46.4°, 57.8°, 62.7°, 66.7° and 69.4° appeared in NCPE films due to dispersion of ZnO nanoparticles, while peaks at 27°, 39° and 56° appeared in NCPE films due to dispersion of TiO₂ nanoparticles, confirms formation of complex. The interaction of nano-sized filler particles with polymer matrix lead to decrease in intermolecular interactions among the polymer chain, this will decrease in crystalline nature of polymer electrolyte. Reduction in crystallinity was studied with the help of crystallite size (L), obtained from using Scherrer’s relation: $L = c\lambda/\beta \cos \theta$, where c is Scherrer’s

constant, λ the X-ray wavelength, β the full-width half-maxima (FWHM) and θ Bragg diffraction angle [23]. Crystallite sizes obtained were 47 nm for SPE and 20 and 30 nm for 3 wt% of ZnO or TiO₂ nanoparticles dispersed in 70PVDF:30Mg(NO₃)₂, respectively.

3.3 Temperature dependence of conductivity and activation energy

Figure 3a shows Log σ vs. $1/T$ plot of SPE and NCPE films with various concentrations of ZnO or TiO₂ nanoparticles in SPE. From figure 3a it was observed that all, plots are linear in nature so these were explained by Arrhenius equation, i.e., $\sigma = \sigma_0 \exp(E_a/k_B T)$, where σ is ionic conductivity, σ_0 the pre-exponential factor, E_a the activation energy, k_B the Boltzmann constant and T temperature, respectively [35–38]. Conductivity value increased from 5.22×10^{-5} S cm⁻¹ (RT) to 3.7×10^{-4} S cm⁻¹ (120°C) of OCC of NCPE, i.e., 70PVDF:30Mg(NO₃)₂:3ZnO and 1.01×10^{-5} S cm⁻¹ (RT) to 2.9×10^{-4} S cm⁻¹ for 3 wt% TiO₂ dispersed in SPE system. Figure 3b shows composition dependence of activation energy (E_a). The activation energy values obtained for SPE (~0.45 eV) and NCPE were 0.29 and 0.30 eV for 3 wt% ZnO or TiO₂ nanoparticles dispersed in SPE, respectively.

3.4 Dielectric analysis

Dielectric properties in any material may be due to ionic, electronic, dipole orientation and space charge polarization effect. Dielectric behaviour of material is expressed by the equation i.e., $\varepsilon = \varepsilon' (= C_p t/\varepsilon_0 A) + j\varepsilon'' (= \sigma/\omega\varepsilon) = 1/j\omega CZ$. ε'

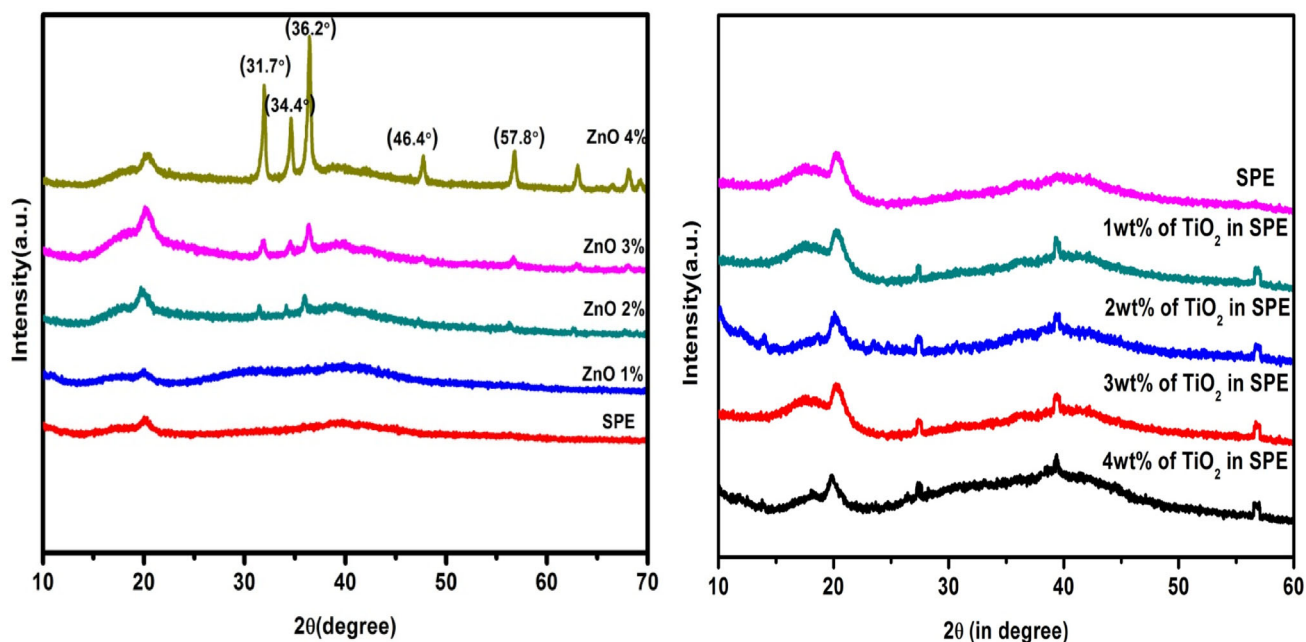


Figure 2. XRD patterns of SPE and NCPEs with composition 70PVDF:30Mg(NO₃)₂:*x* wt% of ZnO or TiO₂ (where *x* = 1, 2, 3 and 4 in wt%).

is real part (dielectric constant) and ε'' is imaginary part (dielectric loss) of dielectric constant, Z the complex impedance, C the capacitance of a material, C_p the parallel capacitance, t the distance between electrodes and A the area of sample, σ the ionic conductivity and ω represents angular frequency. Figure 4a shows variation of real part of dielectric constant with frequency and figure 4b shows variation of imaginary part of dielectric constant with frequency at different temperatures for OCC of NCPE 70PVDF:30Mg(NO₃)₂:3ZnO (30 to 120°C) and 70PVDF:30Mg(NO₃)₂:3TiO₂ (303 to 383 K). It was observed that variation of dielectric constant with frequency at different temperatures is just reverse of variation of electrical conductivity with frequency. Value of dielectric constant decreases on increase in frequency and is saturated at higher frequencies, this may be due to inability of dipoles rapid rotation or electrical relaxation. The high value of dielectric constant at low frequency may contribute to motion of ions; this causes high conductivity of material [39,40]. From figures, it was observed that dielectric constant value increased with increase in temperature of polymer electrolyte (due to increase in concentration of free charges on raising the temperature of electrolyte).

3.5 Studies on ionic conductivity of PVDF:Mg(NO₃)₂:Al₂O₃ NCPEs

Figure 5a shows 'Log σ - x ' plot of NCPE thin films with varying concentrations of Al₂O₃ nanoparticles in 70PVDF:30Mg(NO₃)₂ at room temperature to improve in its conductivity value. The

enhancement in the ionic conductivity value ($\sigma_{rt} = 9.5 \times 10^{-6}$ S cm⁻¹) was observed for 2 wt% of Al₂O₃ dispersed in 70PVDF:30Mg(NO₃)₂ ($\sigma_{rt} = 7.3 \times 10^{-8}$ S cm⁻¹) polymer electrolyte system. Figure 5b shows XRD patterns of SPE i.e., 70PVDF:30Mg(NO₃)₂ and NCPE thin films at various concentrations of Al₂O₃ in SPE. From XRD patterns of NCPE film, it was observed that a broad peak around 20.3° found to decrease in intensity and peaks at 23°, 36.9°, 44.4° and 58.3° appeared in NCPE films due to dispersion of Al₂O₃ nanoparticles; this confirms the formation of complex. Figure 5c shows Log σ vs. $1/T$ plot of SPE and NCPE films with various concentrations of Al₂O₃ nanoparticles in SPE at different temperatures and it was observed that as temperature of polymer electrolyte increases polymer is expanded and produces free volume, which enhances ion transport and increases in conductivity. Conductivity value increased from 9.5×10^{-6} S cm⁻¹ (RT) to 1.01×10^{-4} S cm⁻¹ (120 °C) of OCC of NCPE i.e., 70PVDF:30Mg(NO₃)₂:2Al₂O₃. Figure 5d shows composition dependence of activation energy (E_a). Figure 5e shows variation of real part of dielectric constant with frequency and figure 5f shows variation of imaginary part of dielectric constant with frequency at different temperatures for OCC of NCPE 70PVDF:30Mg(NO₃)₂:2Al₂O₃.

3.6 FTIR studies

FTIR is an important technique that analyses the chain structure of polymer and ion-polymer interactions at molecular level. The vibrational bands of FTIR spectra

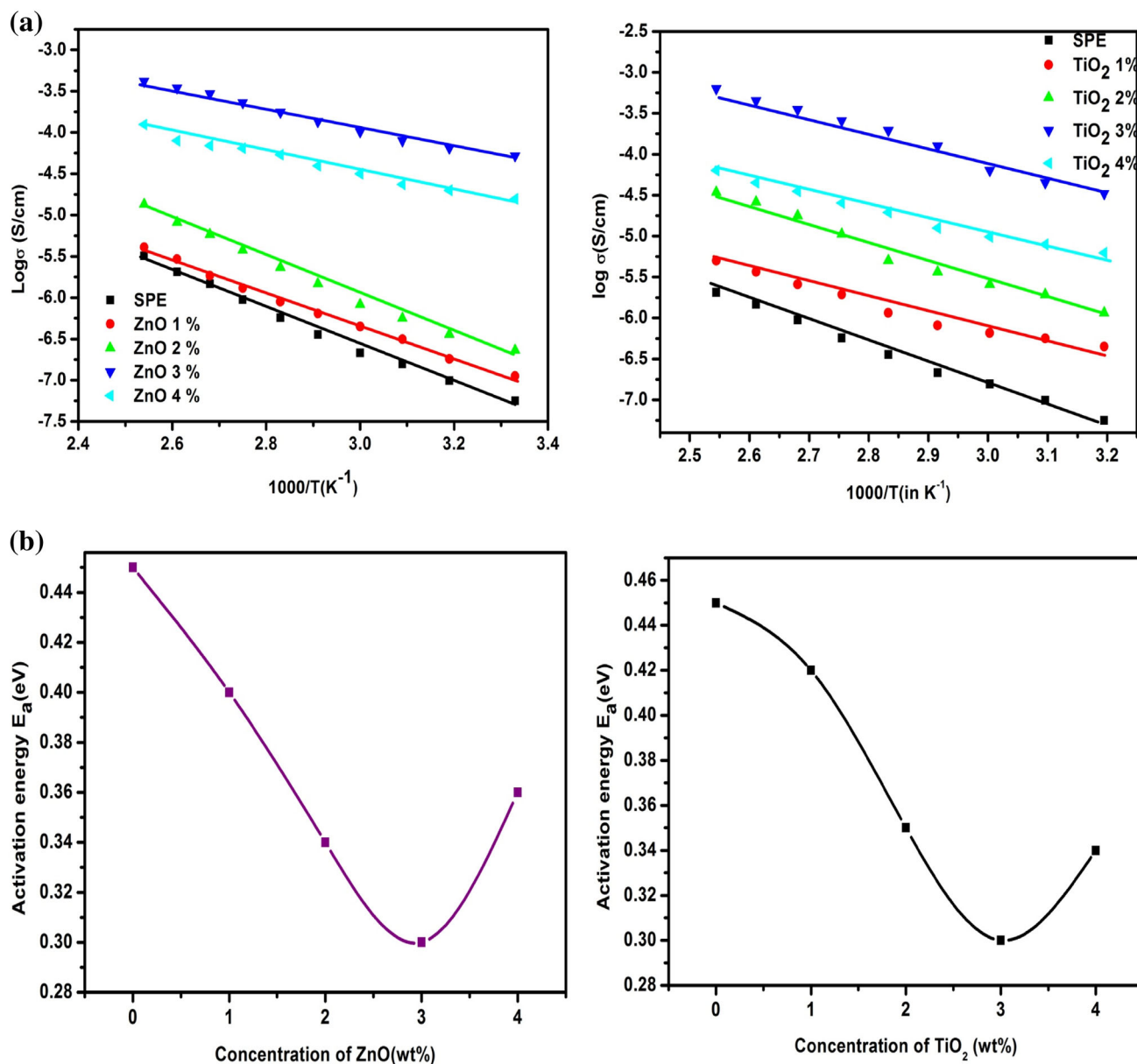


Figure 3. (a) Log σ vs. $1/T$ plot of SPE and NCPE films with various concentrations of ZnO or TiO₂ nanoparticles in SPE at different temperatures. (b) Activation energy vs. x wt% of ZnO or TiO₂ nano-filler concentration dispersed in SPE.

results from vibrational motion of individual bonds or group in a molecule. Any change occurring in bonding situation of molecule (polymer chain) results in change in vibrational frequency position of prominent characteristic bands appearing in the spectra [24]. Positions of peaks present in PVDF are listed in table 1. FTIR spectra of pure polymer, ionic salt, SPE and NCPE thin films with various compositions of nanoparticles are shown in figure 6. It was observed from FTIR spectra of SPE, peak shifted from 1386.00 to 1396.00 cm⁻¹ due to -C-F-Mg interaction, this shifting of peak may be due to addition of salt into pure PVDF, hence formation of complex confirmed or ion polymer interaction takes place. In case of FTIR spectra of NCPE, peak intensity diminished at 1208.00 cm⁻¹ due to

-CF₂-Mg-nanoparticles interaction (asymmetrical stretching). On dispersing nanoparticles into SPE, no significant changes were observed in terms of appearance of new peaks or absence of existing peaks, only intensity of peaks 548.00, 970.00, 1208.00 and 2358.00 cm⁻¹ was decreased confirming the formation of complex [41].

3.7 Transport number studies

The ionic (t_{ion}) and electronic (t_{ele}) transport number were measured by applying a constant dc voltage of 2.5 V across the cell fabricated in configuration Mg|NCPE|IC at room

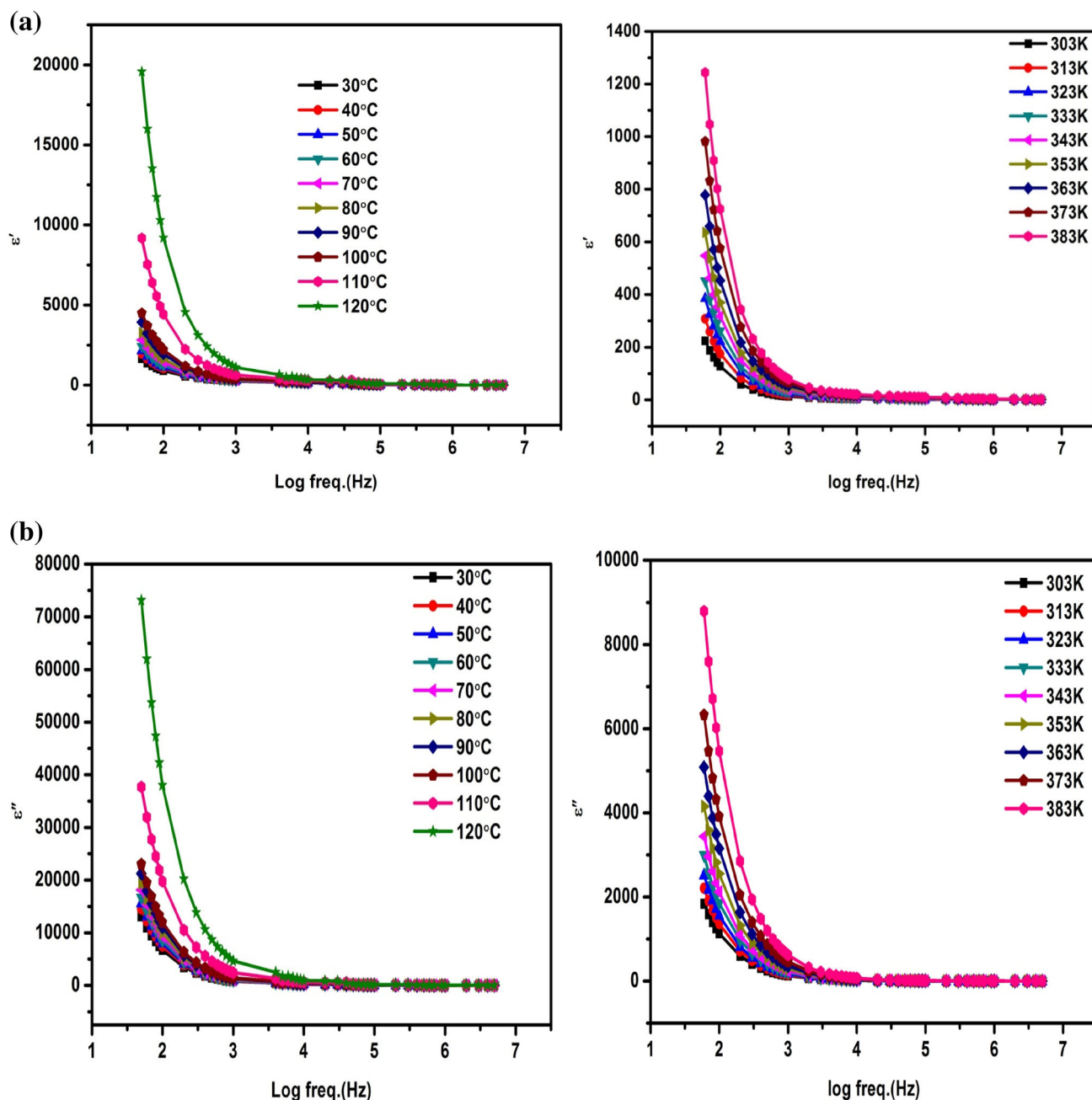


Figure 4. Variations of (a) real part and (b) imaginary part of dielectric constant as a function of frequency of the OCC of NCPE:70PVDF:30Mg(NO₃)₂:3ZnO and 70PVDF:30Mg(NO₃)₂:3TiO₂.

temperature [42]. Figure 7 shows (polarization current vs. time plots) that the polarization current is large in the beginning but as time goes on the current decays immediately and approaches steady state (after some time of polarization before stabilizing at lower level). Transport number of electrolyte gives quantitative information of extent of ionic and electronic contribution to the total conductivity. The t_{ion} value obtained from current vs. time plot for SPE (~ 0.96) and NCPE (~ 0.99) for optimum compositions of nanoparticles dispersed in SPE,

respectively, which is nearly unity, indicating that the nature of the electrolyte is ionic.

3.8 Discharge studies

The discharge characteristics of electrochemical cell gives information about cell parameters as a function of time with cell configuration Mg|NCPE|C-cell (C+I₂+electrolyte, 5:5:1) for NCPE dispersed with various nanoparticles and discharge

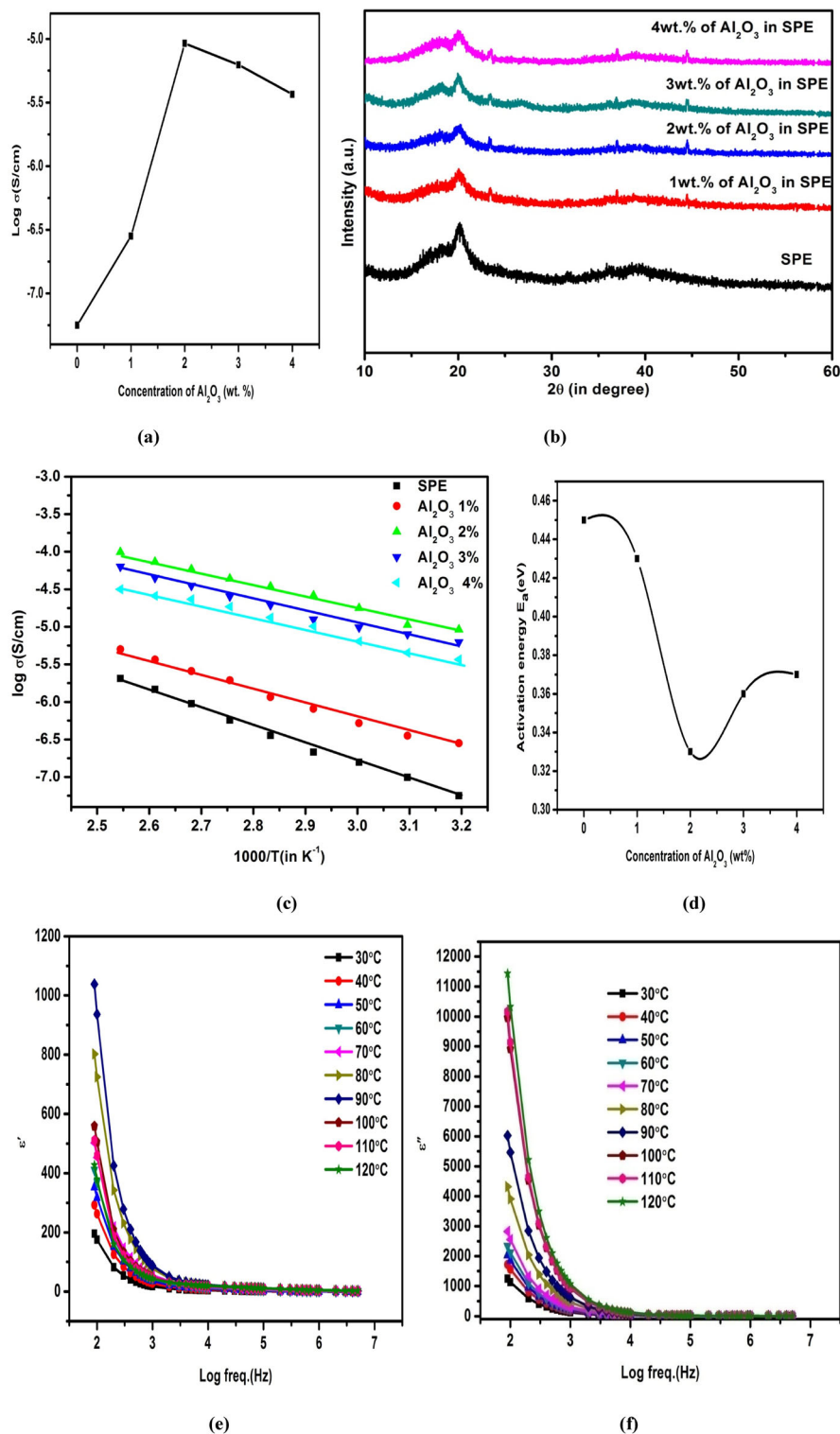
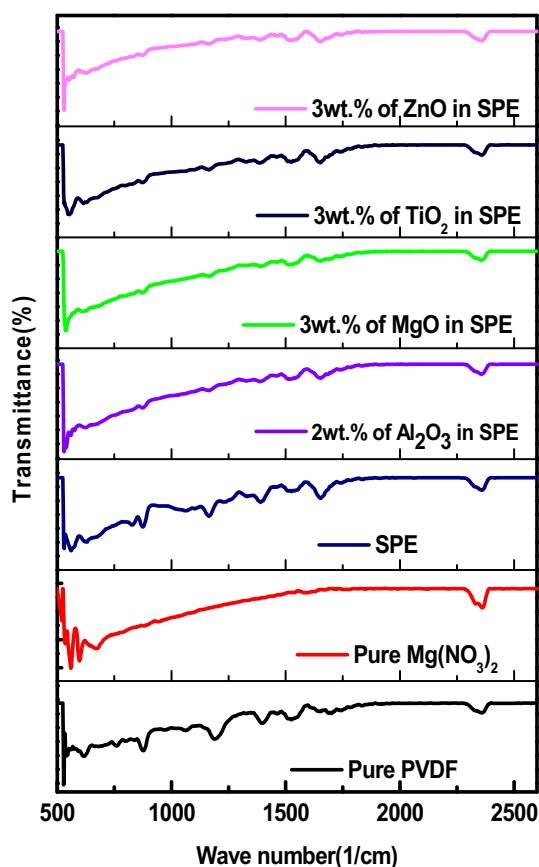


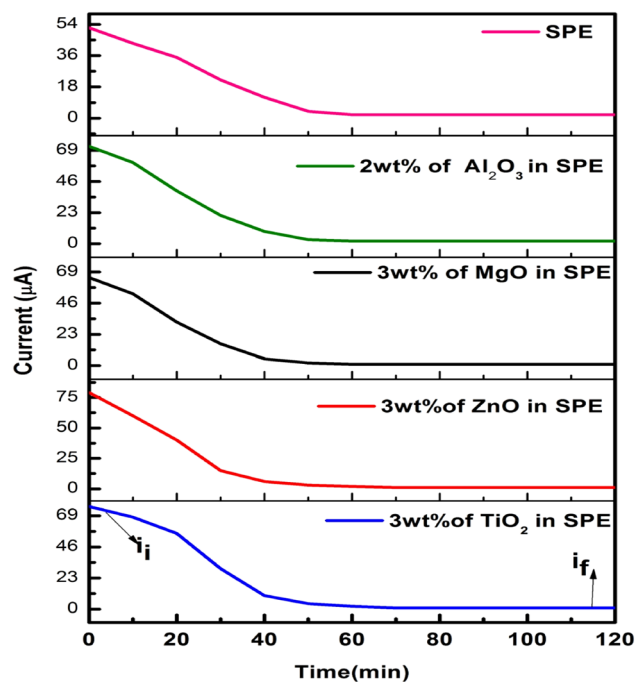
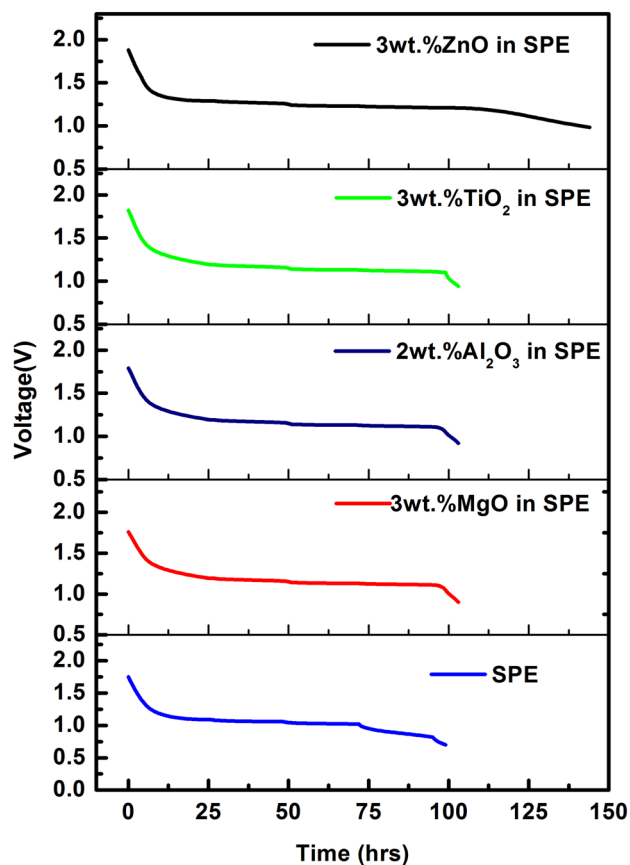
Figure 5. (a) $\text{Log } \sigma$ vs. x plot of SPE and NCPE films with various concentrations of Al₂O₃ nanoparticles in SPE at room temperatures and (b) XRD patterns of SPE and NCPE. (c) $\text{Log } \sigma$ vs. $1000/T$ plot of SPE and NCPE films with various concentrations of Al₂O₃ nanoparticles in SPE at different temperatures. (d) Activation energy vs. x wt% of Al₂O₃ dispersed in SPE. Variation of (e) real part and (f) imaginary part of dielectric constant as a function of frequency for PVDF:Mg(NO₃)₂:Al₂O₃ (70:30:2) NCPE system at different temperatures.

Table 1. Assignment of important FTIR bands in PVDF.

IR bands (cm^{-1})	Possible assignments	References
2358.42	CH_2 symmetric stretching	[24]
1400.00	CH_2 wagging of PVDF	[36]
1387.00	C–F stretching	[41]
1208.00	Asymmetrical stretching of $-\text{CF}_2-$	[41]
1175.00	Symmetrical stretching of $-\text{CF}_2-$	[41]
1068.00	C–C skeletal vibration	[41]
876.00	Strong amorphous phase	[41]
834.00, 812.00	Alpha phase of PVDF	[36]
774.00	Alpha phase of PVDF	[36]
548.00	CF_2 bending	[24]

**Figure 6.** FTIR patterns for pure PVDF, salt, SPE and NCPE with various concentrations of nanoparticles, i.e., PVDF: $\text{Mg}(\text{NO}_3)_2$: x wt% of nanoparticles (where $x = 1, 2, 3$ and 4 in wt%).

at $100 \text{ k}\Omega$. It was observed from figure 8 that initial sharp decrease in voltage with time may be due to polarization or formation of thin layer of magnesium salt at electrode–electrolyte interface [43]. The cell parameters such as an open circuit potential (OCP), current density, energy and power

**Figure 7.** Current vs. time plot of SPE, i.e., 70PVDF:30 $\text{Mg}(\text{NO}_3)_2$ and NCPE with different compositions of nanoparticles in SPE in test cell configuration Mg|NCPE|C.**Figure 8.** Discharge characteristic of SPE, i.e., 70PVDF:30 $\text{Mg}(\text{NO}_3)_2$ and NCPE dispersed with nanoparticles in SPE in electrochemical cell Mg|NCPE|C-cell at $100 \text{ k}\Omega$.

density, etc. were calculated. For all the samples, area of cell is constant, i.e., 1.33 cm^2 . For the OCC of NCPE system, i.e., 70PVDF:30Mg(NO₃)₂:3ZnO has OCP = 1.85 V, current density = $81.91 \mu\text{A cm}^{-2}$, energy and power density are 33 Wh kg^{-1} and 0.33 W kg^{-1} , respectively.

4. Conclusions

NCPEs dispersed with various concentrations of ZnO, TiO₂ and Al₂O₃ nanoparticles in SPE 70PVDF:30Mg(NO₃)₂ have been synthesized by using solution cast technique. The XRD and FTIR studies confirm formation of complex. Composition and temperature-dependent ionic conductivity studies among all three systems gives highest ionic conductivity for 70PVDF:30Mg(NO₃)₂:3ZnO system, i.e., $\sigma = 5.22 \times 10^{-5} \text{ S cm}^{-1}$ at room temperature and $3.7 \times 10^{-4} \text{ S cm}^{-1}$ at 120°C with lowest activation energy $\sim 0.29 \text{ eV}$. This system has transference number $t_{\text{ion}} = 0.99$, which shows that nature of electrolyte is ionic. This NCPE system also has maximum dielectric constant observed from temperature-dependent dielectric studies. From battery performance of all electrolytes, 70PVDF:30Mg(NO₃)₂:3ZnO system has highest OCV (1.85 V), which suggests that this system can be suitable candidate for fabrication of electrochemical devices in near future.

Acknowledgements

We gratefully acknowledge the kind support of Department of Chemistry of Dr Harisingh Gour Vishwavidyalaya for providing the facility of Impedance analyzer and FTIR spectrophotometer. One of the authors Nidhi is thankful to the UGC Fellowship, for the financial assistance.

References

- [1] Pu W, He X, Wang L, Jiang C and Wan C 2006 *J. Membr. Sci.* **272** 11
- [2] Agrawal R C, Chandra A, Mahipal Y K and Beena R 2008 *Proc. 11th ACSSSI (Coimbatore, India)* B V R Chowdari *et al* (ed) (New Delhi: Macmillan) **577**
- [3] Nidhi, Patel S and Kumar R 2020 *ICC-2019 AIP Conf. Proc.* **2220** 080044
- [4] Singh J T and Bhat S V 2003 *Bull. Mater. Sci.* **26** 707
- [5] Manoravi P, Selvaraj I, Chandrasekhar V and Shahi K 1993 *Polymer* **34** 1339
- [6] Scrosati B 1995 *Nature* **373** 55
- [7] Shi Q, Yu M, Zhou X and Wan C 2002 *J. Power Sources* **103** 286
- [8] Wu C G, Lu M and Chuang H J 2005 *Polymer* **46** 5929
- [9] Zhang R, Tutusau O, Mohtadi S R and Ling C 2018 *Front. Chem.*, <https://doi.org/10.3389/fchem.2018.00611>
- [10] Song J Y, Cheng C L, Wang Y Y and Wan C C 2002 *J. Electrochem. Soc.* **149** A1230
- [11] Sundaram N T K and Subramania A 2007 *J. Membr. Sci.* **289** 1
- [12] Polu A R, Kumar R, Causin V and Neppalli R 2011 *J. Korean Phys. Soc.* **59** 114
- [13] Nidhi, Patel S and Kumar R 2019 *J. Alloys Compd.* **789** 6
- [14] Damle R, Kulkarni P N and Bhat S V 2008 *Bull. Mater. Sci.* **31** 869
- [15] Armand M B, Chabagno J M, Duclot M J, Mundy J N and Shenoy G K 1979 *Fast ion transport in solids* (New York: Elsevier) p 131
- [16] Money B K, Hariharan K and Swenson J 2014 *Solid State Ion.* **262** 785
- [17] Polu A R and Kumar R 2012 *AIP Conf. Proc.* **1447** 969
- [18] Polu A R and Kumar R 2013 *Adv. Mater. Lett.* **4** 543
- [19] Pandey G P and Hashmi S A 2009 *Electroactive polymer: materials and devices* Vol 3 (India: Macmillan Publishers) p 131
- [20] Wieczorek W, Stevens J R and Florjanczyk Z 1996 *Solid State Ion.* **85** 67
- [21] Priya H H G, Suganya N and Jaisankar V 2015 *IJCRGG* **7** 2942
- [22] Johnsi M and Suthanthiraraj S A 2016 *Ionics*, <https://doi.org/10.1007/s11581-016-1637-x>
- [23] Prabakaran P, Prabhu R, Manimuthu and Gurusamy S 2016 *J. Solid State Electrochem.*, <https://doi.org/10.1007/s10008-016-3477-z>
- [24] Hema M, Tamilselvi P and Hirankumar G 2016 *Ionics*, <https://doi.org/10.1007/s11581-016-1925-5>
- [25] Saikia D, Chen Y Y W, Chen Y T, Li Y K and Lin S I 2008 *Desalination* **234** 24
- [26] Reddy C V S, Sharma A K and Rao V V R N 2006 *Polymer* **47** 1318
- [27] Pandey G P, Hashmi S A and Agrawal R C 2008 *J. Phys. D: Appl. Phys.* **41** 055409
- [28] Reddy M J, Sreekanth T, Chandrasekhar M and Rao U V S 2000 *J. Mater. Sci.* **35** 2841
- [29] Sharma M N V D, Sarma A V and Rao R B 2009 *J. Mater. Sci.* **47** 5557
- [30] Shalu, Balo L, Gupta H, Singh V K and Singh R K 2016 *RSC Adv.* **6** 73028
- [31] Pradeepa P, Edwinraj S and Prabhu M R 2015 *Chinese Chem. Lett.* **26** 1191
- [32] Knight J C, Therese S and Manthiram A 2015 *ACS Appl. Mater. Interfaces*, <https://doi.org/10.1021/acsami.5b06179>
- [33] Magistris A, Schiraldi A and Chiodelli G 1977 *Electrochem. Acta* **22** 689
- [34] Ratner M A and Shriver D F 1988 *Chem. Rev.* **88** 109
- [35] Prabakaran K, Mohanty S and Nayak S K 2015 *J. Solid State Electrochem.* **19** 2465
- [36] Mishra K, Hashmi S A and Rai D K 2014 *J. Solid State Electrochem.* **18** 2255
- [37] Miyamoto T and Shibayama K 1973 *J. Appl. Phys.* **44** 5372
- [38] Aziz S B, Woo T J, Kadir M F Z and Ahmed H M 2018 *J. Sci.: Adv. Mater. Devices* **3** 1
- [39] Kumar T V, Chary A, Bhardwaj S, Awasthi A M and Reddy S N 2013 *Int. J. Mater. Sci. Appl.* **2** 173
- [40] Tripathi S K, Gupta A, Jain A and Kumari M 2013 *Indian J. Pure Appl. Phys.* **51** 358
- [41] Ramesh S and Lu S C 2011 *J. Mol. Struct.* **994** 403
- [42] Wagner A K and Wagner C 1957 *J. Chem. Phys.* **26** 1597
- [43] Basha S K S, Sundari G S and Kumar K V 2015 *Int. J. Chem. Tech. Res.* **2** 803